Above-threshold multiphoton detachment of H^- by two-color laser fields: Angular distributions and partial rates

Dmitry A. Telnov,* Jingyan Wang, and Shih-I Chu
Department of Chemistry, University of Kansas, Lawrence, Kansas 66045
(Received 17 November 1994)

We present a general nonperturbative formalism and an efficient and accurate numerical technique for the study of the angular distributions and partial widths for multiphoton above-threshold detachment in two-color fields. The procedure is based on an extension of our recent paper [D. A. Telnov and S.-I Chu, Phys. Rev. A **50**, 4099 (1994)] for one-color detachment, and the many-mode Floquet theory [T. S. Ho, S.-I Chu, and J. V. Tietz, Chem. Phys. Lett. **96**, 464 (1983)]. The generalization of this procedure is performed for both cases of commensurable and incommensurable frequencies of the two-color fields. The procedure consists of the following elements: (i) Determination of the resonance wave function and complex quasienergy by means of the non-Hermitian Floquet Hamiltonian formalism. The Floquet Hamiltonian is discretized by the complex-scaling generalized pseudospectral technique recently developed [J. Wang, S.-I Chu, and C. Laughlin, Phys. Rev. A **50**, 3208 (1994)]. (ii) Calculation of the angular distribution and partial widths based on an exact differential formula and a procedure for the rotation of the resonance wave function back to the real axis. The method is applied to a nonperturbative study of multiphoton above-threshold detachment of H^- by 10.6-μm radiation and its third harmonic (the commensurable case). The results show strong dependence on the relative phase δ between the fundamental frequency field and its harmonic. For the intensities used in calculations (10^{10} W/cm^2 for the fundamental frequency, 10^8 and 10^9 W/cm^2 for the harmonic), the total rate has its maximum at $\delta=0$ and minimum at $\delta=\pi$. However, this tendency, though valid for the first several above-threshold peaks in the energy spectrum, is reversed for the higher-energy peaks. The energy spectrum for $\delta=\pi$ is broader, and the peak heights decrease more slowly compared to the case of $\delta=0$. The strong phase dependence is also manifested in the angular distributions of the ejected electrons.

PACS number(s): 32.80.Rm, 32.80.Fb, 42.50.Hz

I. INTRODUCTION

Recent experiments on above-threshold ionization with two-color laser fields [1] have stimulated considerable theoretical investigation. Several nonperturbative calculations were performed in recent years. Schafer and Kulander [2] presented time-dependent calculations of above-threshold ionization of atomic hydrogen by the fundamental radiation field and its second harmonic. They found that using different wavelengths of the fundamental field leads to a qualitative change in the ionization dynamics. At longer wavelengths the total ionization rate is determined by the peak instantaneous electric field; this is a characteristic of the tunneling ionization regime. At shorter wavelengths, the interference between different multiphoton excitation pathways, and not the electric field peak value, plays a key role. However, the partial rates show considerable structure dependent on the relative phase between the two fields in both cases. Also, for atomic hydrogen, Potvliege and Smith in a series of papers [3–5] used the time-independent Floquet method for the determination of the total rates using in calculations the frequency ratios 1:2, 1:3, and 2:3. For the ratio 1:3 [i.e., for the fundamental field and its third harmonic with the time dependences $\cos(\omega t)$ and $\cos(3\omega t+\delta)$, respectively], they found a dramatic increase of the total ionization rate by the two-color field compared to one-color ionization by the fundamental frequency field, in a wide range of the intensities of the harmonic field [3]. The rate is increased for all relative phase δ values, being the greatest for $\delta=0$. However, for $\delta=\pi$ and the harmonic field much weaker than the fundamental one (10^{-4} times in intensity and below) the rate in fact becomes significantly less than that for the fundamental field alone. Further, the relative phase dependence of the total rates is more pronounced for the frequency ratio 1:3 than for 1:2 [4] and 2:3 [5] since all the pathways leading to a continuum states with the same energy interfere in the 1:3 case whereas a considerable pattern of uninterfering pathways exists for the other cases due to parity or energy restrictions [5]. The oscillatory ionization probability dependence on the relative phase with the maximum at $\delta=0$ and minimum at $\delta=\pi$ was also reported by Pont, Proulx, and Shakeshaft [6] for the 1:3 case in time-dependent pulse calculations.

The theoretical papers cited above deal with atomic hydrogen. Recently there is also much interest in the study of multiphoton detachment of negative atomic ions (mainly H^-) both experimentally [7–9] and theoretically [10–12]. Due to short-range interaction between the

*Permanent address: Institute of Physics, St. Petersburg State University, 198904 St. Petersburg, Russia. Electronic address: photon94@kuhub.cc.ukans.edu

outer electron and the core, the H^- negative ions possess only one bound state. Further, under the current experimental conditions [7–9], doubly excited states far above the ionization threshold can be safely ignored for moderately strong laser fields. These simplifying features render the multiphoton detachment of H^- a unique and fundamental process to study. In our previous paper [13] we presented a theoretical study on the angular distribution and partial widths for multiphoton above-threshold detachment of H^-. Here we extend the approach of Ref. [13] to the case of the two-color field.

The H^- ion is described by an accurate one-electron model recently constructed [11] to reproduce both the exact experimental binding energy [14] and the low-energy e-H($1s$) elastic phase shifts [15]. The one-photon detachment cross sections based on this model potential are in excellent agreement with earlier accurate correlated two-electron calculations [16]. A complex-scaling generalized pseudospectral (CSGPS) technique [12,17] is introduced to discretize and facilitate the solution of the time-independent non-Hermitian Floquet Hamiltonian [18,19] for the complex quasienergies and eigenfunctions. Then the electron energy and angular distributions are calculated using the reverse complex-scaling method developed in Ref. [13].

The motivations and outline of this paper are described as follows. First, we extend our recent nonperturbative study [13] of the angular distributions and partial widths in above-threshold detachment of H^- to the case of a two-color field. The general theory of electron distributions is developed for both commensurable and incommensurable frequencies whereas the calculations are performed for the fundamental frequency of a CO_2 laser (wavelength 10.6 μm) and its third harmonic. Second, the (complex quasienergy) resonance wave functions are obtained by the solution of the non-Hermitian Floquet Hamiltonian and the use of the CSGPS technique. In contrast with Ref. [13], we do not use here further approximations for the wave functions based on the adiabatic theory [20]. The CSGPS procedure does not require the computation of potential matrix elements and is computationally simpler and faster than the conventional basis-set expansion-variational methods. The advantages and usefulness of this method have been discussed in [12,17].

We begin in Sec. II the presentation of the general theory for electron distributions in the two-color case. Section III presents the main numerical results for above-threshold detachment of H^- at 10.6 μm, 10^{10} W/cm^2 laser field and its third harmonic with the intensities 10^8 and 10^9 W/cm^2. This is followed by a conclusion in Sec. IV.

II. THEORY

Let us consider the time-dependent Schrödinger equation for the electron bound in the atomic potential $W(r)$ and subject to the influence of the external two-color laser field (atomic units are used):

$$i\frac{\partial}{\partial t}\Psi(\mathbf{r},t)=\left[-\frac{1}{2}\nabla^2+W(r)+[\mathbf{F}_1\cos\omega_1 t+\mathbf{F}_2\cos(\omega_2 t+\delta)]\cdot\mathbf{r}\right]\Psi(\mathbf{r},t)\ . \tag{1}$$

Equation (1) implies linear polarization for both the fields with the frequencies ω_1 and ω_2, however, the orientation of the field vectors $\mathbf{F}_1$ and $\mathbf{F}_2$ can be arbitrary. δ is the phase difference between the two fields for $t=0$.

We introduce the following notations:

$$\mathbf{a}_1(t)=-\int^t\mathbf{F}_1\cos(\omega_1\tau)d\tau=-\omega_1^{-1}\mathbf{F}_1\sin\omega_1 t\ , \tag{2}$$

$$\mathbf{a}_2(t)=-\int^t\mathbf{F}_2\cos(\omega_2\tau+\delta)d\tau=-\omega_2^{-1}\mathbf{F}_2\sin(\omega_2 t+\delta)\ , \tag{3}$$

$$\mathbf{b}_1=\int^t\mathbf{a}_1(\tau)d\tau=\omega_1^{-2}\mathbf{F}_1\cos\omega_1 t\ , \tag{4}$$

$$\mathbf{b}_2=\int^t\mathbf{a}_2(\tau)d\tau=\omega_2^{-2}\mathbf{F}_2\cos(\omega_2 t+\delta)\ . \tag{5}$$

Here $\mathbf{a}_{1,2}$ are the vector potentials of the laser fields (except c factor, c being the light velocity), and $\mathbf{b}_{1,2}$ have the sense of the classical electron oscillatory displacement due to monochromatic external fields.

A. Incommensurable frequencies

Let us consider first the case of incommensurable frequencies ω_1 and ω_2. In this case the combined external field is not periodic in time, so ordinary Floquet solutions of Eq. (1) do not exist. However, according to the many-mode Floquet theorem [21] one can look for the wave function $\Psi(\mathbf{r},t)$ in the following form:

$$\Psi(\mathbf{r},t)=\exp(-i\varepsilon t)\psi(\mathbf{r},t)\ , \tag{6}$$

where ε is the two-mode quasienergy, and $\psi(\mathbf{r},t)$ is not periodic but quasiperiodic in time, i.e., it can be expanded in a double Fourier series with two fundamental frequencies:

$$\psi(\mathbf{r},t)=\sum_{m_1,m_2}\psi_{m_1m_2}(\mathbf{r})\exp[-i(m_1\omega_1 t+m_2\omega_2 t)]\ . \tag{7}$$

The function $\psi(\mathbf{r},t)$ satisfies the following equation:

$$i\frac{\partial\psi}{\partial t}=\left[-\frac{1}{2}\nabla^2+W(r)+[\mathbf{F}_1\cos\omega_1 t+\mathbf{F}_2\cos(\omega_2 t+\delta)]\cdot\mathbf{r}-\varepsilon\right]\psi\ , \tag{8}$$

which is equivalent to the infinite set of time-independent equations for the Fourier components $\psi_{m_1m_2}(\mathbf{r})$:

$$[-\tfrac{1}{2}\nabla^2+W(r)-E_{m_1m_2}]\psi_{m_1m_2}+\tfrac{1}{2}\{(\mathbf{F}_1\cdot\mathbf{r})[\psi_{m_1-1,m_2}+\psi_{m_1+1,m_2}]+(\mathbf{F}_2\cdot\mathbf{r})[\exp(-i\delta)\psi_{m_1m_2-1}+\exp(i\delta)\psi_{m_1m_2+1}]\}=0 , \tag{9}$$

where

$$E_{m_1m_2}=\varepsilon+m_1\omega_1+m_2\omega_2 . \tag{10}$$

Now we introduce the function $\psi_2(\mathbf{r},t_1,t_2)$ depending on two time arguments t_1 and t_2. This function is defined by two-time, two-frequency Fourier series with the same coefficients as in Eq. (7):

$$\psi_2(\mathbf{r},t_1,t_2)=\sum_{m_1,m_2}\psi_{m_1m_2}(\mathbf{r})\exp[-i(m_1\omega_1t_1+m_2\omega_2t_2)] . \tag{11}$$

It can be easily verified that the function $\psi_2(\mathbf{r},t_1,t_2)$ satisfies the two-time Schrödinger equation:

$$\left[i\frac{\partial}{\partial t_1}+i\frac{\partial}{\partial t_2}\right]\psi_2(\mathbf{r},t_1,t_2)=\left[-\frac{1}{2}\nabla^2+W(r)+[\mathbf{F}_1\cos\omega_1t_1+\mathbf{F}_2\cos[\omega_2t_2+\delta)]\cdot\mathbf{r}-\varepsilon\right]\psi_2(\mathbf{r},t_1,t_2) . \tag{12}$$

Indeed, using the expression (11) in Eq. (12) and separating the time harmonics we obtain again the set of equations (9) for the Fourier components $\psi_{m_1m_2}(\mathbf{r})$. To obtain the general expressions for the electron distributions after two-color detachment we need to perform a chain of transformations of Eq. (12). First, Eq. (12) accounts for the external field in the length gauge. We need to convert it into the velocity gauge with the help of the following transformation:

$$\psi_2(\mathbf{r},t_1,t_2)=\psi_2^v(\mathbf{r},t_1,t_2)\exp\{i[\mathbf{a}_1(t_1)+\mathbf{a}_2(t_2)]\cdot\mathbf{r}\} . \tag{13}$$

The equation for the function $\psi_2^v(\mathbf{r},t_1,t_2)$ is

$$\begin{aligned}\left[i\frac{\partial}{\partial t_1}+i\frac{\partial}{\partial t_2}\right]\psi_2^v(\mathbf{r},t_1,t_2)=\Bigg[&-\frac{1}{2}\nabla^2+W(r)-i[\mathbf{a}_1(t_1)+\mathbf{a}_2(t_2)]\cdot\nabla\\&+(\omega_1\omega_2)^{-1}\mathbf{F}_1\cdot\mathbf{F}_2\sin(\omega_1t_1)\sin(\omega_2t_2+\delta)-(2\omega_1)^{-2}\mathbf{F}_1^2\cos(2\omega_1t_1)\\&-(2\omega_2)^{-2}\mathbf{F}_2^2\cos(2\omega_2t_2+2\delta)-\varepsilon_v\Bigg]\psi_2^v(\mathbf{r},t_1,t_2) ,\end{aligned} \tag{14}$$

with the quasienergy for the velocity gauge ε_v defined as

$$\varepsilon_v=\varepsilon-(2\omega_1)^{-2}\mathbf{F}_1^2-(2\omega_2)^{-2}\mathbf{F}_2^2 . \tag{15}$$

Then the terms due to the external field in the right-hand side of Eq. (14) can be eliminated by the following transformation of the wave function:

$$\begin{aligned}\psi_2^v(\mathbf{r},t_1,t_2)=\psi_2^q(\mathbf{R},t_1,t_2)\exp\{&i(2\omega_1)^{-3}\mathbf{F}_1^2\sin2\omega_1t_1+i(2\omega_2)^{-3}\mathbf{F}_2^2\sin(2\omega_2t_2+2\delta)\\&+i(2\omega_1\omega_2)^{-1}\mathbf{F}_1\cdot\mathbf{F}_2[(\omega_1+\omega_2)^{-1}\sin(\omega_1t_1+\omega_2t_2+\delta)-(\omega_1-\omega_2)^{-1}\sin(\omega_1t_1-\omega_2t_2-\delta)]\} ,\end{aligned} \tag{16}$$

where the new coordinate $\mathbf{R}$ is defined as

$$\mathbf{R}=\mathbf{r}-\mathbf{b}_1(t_1)-\mathbf{b}_2(t_2) . \tag{17}$$

The equation for the wave function $\psi_2^q(\mathbf{R},t_1,t_2)$ does not contain the interaction with the external field, but the atomic potential becomes time dependent:

$$\left[i\frac{\partial}{\partial t_1}+i\frac{\partial}{\partial t_2}\right]\psi_2^q(\mathbf{R},t_1,t_2)=\left[-\frac{1}{2}\nabla^2+W(|\mathbf{R}+\mathbf{b}_1(t_1)+\mathbf{b}_2(t_2)|)-\varepsilon_v\right]\psi_2^q(\mathbf{R},t_1,t_2) . \tag{18}$$

Note that the time derivatives in Eq. (18) are taken for the fixed $\mathbf{R}$, and the kinetic energy operator acts on the variable $\mathbf{R}$.

With the help of the quasienergy Green function analogous to that in the one-time theory (see, e.g., Ref. [20]), Eq. (18) is converted into the integral form suitable for further calculations:

$$\psi_2^q(\mathbf{R},t_1,t_2)=-(2\pi)^{-3}\omega_1\omega_2\sum_{n_1,n_2}\exp[-in_1\omega_1t_1-in_2\omega_2t_2]$$
$$\times\int d^3\mathbf{R}'\int_{-\pi/\omega_1}^{\pi/\omega_1}dt_1'\int_{-\pi/\omega_2}^{\pi/\omega_2}dt_2'\exp[in_1\omega_1t_1'+in_2\omega_2t_2']\frac{\exp[ik_{n_1n_2}|\mathbf{R}-\mathbf{R}'|]}{|\mathbf{R}-\mathbf{R}'|}$$
$$\times W(|\mathbf{R}'+\mathbf{b}_1(t_1')+\mathbf{b}_2(t_2')|)\psi_2^q(\mathbf{R}',t_1',t_2')\ . \tag{19}$$

Here

$$k_{n_1n_2}=\sqrt{2(\varepsilon_v+n_1\omega_1+n_2\omega_2)} \tag{20}$$

has the sense of the electron drift momentum after absorption of n_1 photons of frequency ω_1 and n_2 photons of frequency ω_2, for $\mathrm{Re}k_{n_1n_2}^2>0$. For $\mathrm{Re}k_{n_1n_2}^2<0$ one should choose $\mathrm{Im}k_{n_1n_2}^2>0$ to ensure zero boundary conditions at infinity.

The electron energy and angular distributions are extracted from Eq. (19) by calculating the electron flux densities for each set n_1,n_2 such as $\mathrm{Re}k_{n_1n_2}^2>0$:

$$\frac{d\Gamma_{n_1n_2}}{d\Omega}=(2\pi)^{-2}k_{n_1n_2}|A_{n_1n_2}|^2\ , \tag{21}$$

where

$$A_{n_1n_2}=(2\pi)^{-2}\sum_{m_1,m_2}\exp[i(m_2-n_2)\delta]$$
$$\times\int_{-\pi}^{\pi}d\tau_1\int_{-\pi}^{\pi}d\tau_2\exp\{i(n_1-m_1)\tau_1+i(n_2-m_2)\tau_2-i(2\omega_1)^{-3}\mathbf{F}_1^2\sin2\tau_1$$
$$-i(2\omega_2)^{-3}\mathbf{F}_2^2\sin2\tau_2+ik_{n_1n_2}\hat{\mathbf{r}}\cdot(\omega_1^{-2}\mathbf{F}_1\cos\tau_1+\omega_2^{-2}\mathbf{F}_2\cos\tau_2)$$
$$-i(2\omega_1\omega_2)^{-1}\mathbf{F}_1\cdot\mathbf{F}_2[(\omega_1+\omega_2)^{-1}\sin(\tau_1+\tau_2)-(\omega_1-\omega_2)^{-1}\sin(\tau_1-\tau_2)]\}$$
$$\times\int d^3\mathbf{r}'\exp[-ik_{n_1n_2}\hat{\mathbf{r}}\cdot\mathbf{r}'+i\mathbf{r}'\cdot(\omega_1^{-1}\mathbf{F}_1\sin\tau_1+\omega_2^{-1}\mathbf{F}_2\sin\tau_2)]W(r')\psi_{m_1m_2}(\mathbf{r}') \tag{22}$$

is the photodetachment amplitude for the electron ejected in the direction of the unit vector $\hat{\mathbf{r}}$ after absorption of n_1 photons of frequency ω_1 and n_2 photons of frequency ω_2. In the right-hand side of Eq. (22) we turned back to the wave function in the length gauge $\psi_2(\mathbf{r},t_1,t_2)$ performing the inverse transformations and used the Fourier expansion (11). Expression (22) clearly shows that in the case of incommensurable frequencies the electron distributions do not depend on the relative phase shift δ (which is not well defined itself since it can have arbitrary value depending on the initial time moment). Indeed, as one can see from Eq. (9), the dependence of $\psi_{m_1m_2}(\mathbf{r})$ on δ is reduced to the factor $\exp(-im_2\delta)$. Then the amplitude $A_{n_1n_2}$ depends on δ via the phase factor $\exp(-in_2\delta)$ with the absolute value equal to unity, so the differential flux $d\Gamma_{n_1n_2}/d\Omega$ does not depend on the shift δ. This result means that the two-mode Floquet theory has no direct limit to the case of commensurable frequencies (and, in particular, for $\omega_2\to\omega_1$) where the phase shift δ is important. The two-mode Floquet theory treats all the time harmonics with the energies $E_{m_1m_2}=\varepsilon+m_1\omega_1+m_2\omega_2$ as independent, and it is not the case for commensurable frequencies. For example, when ω_2 is very close to ω_1 one needs a very long time to resolve near degenerate time harmonics. So, it may be said that the two-mode Floquet theory in the case of near commensurable frequencies describes a long-time-scale behavior of the system under consideration whereas the one-mode theory describes short and moderate time scales. This is the reason of discrepancies between two-mode and one-mode Floquet theories in the limit of commensurable frequencies.

B. Commensurable frequencies

Now we turn to the case of commensurable frequencies and consider the case when ω_2 is a harmonic of ω_1:

$$\omega_1=\omega,\quad \omega_2=p\omega\ , \tag{23}$$

where p is an integer number. We can use the conventional Floquet theory since the Hamiltonian is now periodic in time. The wave function $\psi(\mathbf{r},t)$ is expanded in the Fourier series with one fundamental frequency ω:

$$\psi(\mathbf{r},t)=\sum_m\psi_m(\mathbf{r})\exp(-im\omega t)\ , \tag{24}$$

and the set of equations for the functions $\psi_m(\mathbf{r})$ reads as

$$\left[-\frac{1}{2}\nabla^2+W(r)-E_m\right]\psi_m+\frac{1}{2}\{(\mathbf{F}_1\cdot\mathbf{r})[\psi_{m-1}+\psi_{m+1}]$$
$$+(\mathbf{F}_2\cdot\mathbf{r})[\exp(-i\delta)\psi_{m-p}+\exp(i\delta)\psi_{m+p}]\}=0\ , \tag{25}$$

with

TABLE I. Partial rates for the detachment by 10.6-μm radiation and its third harmonic with the intensities $I_L = 10^{10}$ W/cm^2 and $I_H = 10^9$ W/cm^2, respectively. The number of photons absorbed refers to the fundamental frequency, for the harmonic field it should be divided by 3. The number in brackets indicates the power of 10.

Number of photons absorbed	One-color fundamental (a.u.)	Two-color (a.u.)				One-color harmonic (a.u.)
		$\delta=0$	$\delta=\pi$	$\delta=\pi/2$	$\delta=-\pi/2$	
8	0.72[−9]	0.42[−7]	0.58[−8]	0.20[−7]	0.21[−7]	
9	0.20[−9]	0.10[−7]	0.23[−8]	0.71[−8]	0.73[−8]	0.30[−10]
10	0.39[−10]	0.26[−8]	0.27[−8]	0.35[−8]	0.30[−8]	
11	0.40[−11]	0.72[−9]	0.16[−8]	0.15[−8]	0.10[−8]	
12	0.71[−12]	0.20[−9]	0.71[−9]	0.58[−9]	0.30[−9]	0.86[−13]
13	0.33[−12]	0.53[−10]	0.27[−9]	0.20[−9]	0.85[−10]	
14	0.14[−12]	0.14[−10]	0.97[−10]	0.69[−10]	0.32[−10]	
15	0.47[−13]	0.32[−11]	0.33[−10]	0.23[−10]	0.17[−10]	0.31[−15]
16	0.14[−13]	0.72[−12]	0.12[−10]	0.78[−11]	0.10[−10]	
17	0.35[−14]	0.22[−12]	0.43[−11]	0.27[−11]	0.60[−11]	
Total rate	0.96[−9]	0.56[−7]	0.14[−7]	0.33[−7]	0.33[−7]	0.30[−10]

$$E_m = \varepsilon + m\omega \ . \tag{26}$$

Performing the same transformations as in the case of incommensurate frequencies but within the one-time approach we obtain the following result for the differential electron flux $d\Gamma_n/d\Omega$:

$$\frac{d\Gamma_n}{d\Omega} = (2\pi)^{-2} k_n |A_n|^2 \ , \tag{27}$$

where

$$k_n = \sqrt{2(\varepsilon_v + n\omega)}, \quad \varepsilon_v = \varepsilon - (2\omega)^{-2}\mathbf{F}_1^2 - (2p\omega)^{-2}\mathbf{F}_2^2 \tag{28}$$

and

$$\begin{aligned} A_n = (2\pi)^{-1} \int_{-\pi}^{\pi} d\tau \exp(& in\tau - i(2\omega)^{-3}\mathbf{F}_1^2 \sin 2\tau - i(2p\omega)^{-3}\mathbf{F}_2^2 \sin(2p\tau + 2\delta) \\ & + ik_n \hat{\mathbf{r}}\cdot[\omega^{-2}\mathbf{F}_1 \cos\tau + (p\omega)^{-2}\mathbf{F}_2 \cos(p\tau+\delta)] \\ & - i(2p\omega^2)^{-1}(\mathbf{F}_1\cdot\mathbf{F}_2)\{[(p+1)\omega]^{-1}\sin[(p+1)\tau+\delta] - [(p-1)\omega]^{-1}\sin[(p-1)\tau+\delta]\}) \\ \times \int d^3\mathbf{r}' \exp\{ & -ik_n \hat{\mathbf{r}}\cdot\mathbf{r}' + i\mathbf{r}'\cdot[\omega^{-1}\mathbf{F}_1 \sin\tau + (p\omega)^{-1}\mathbf{F}_2 \sin(p\tau+\delta)]\} W(r')\psi(\mathbf{r}', \tau/\omega) \ . \end{aligned} \tag{29}$$

Using the Fourier expansion (24) we can obtain another expression for the amplitude A_n:

TABLE II. Partial rates for the detachment by 10.6-μm radiation and its third harmonic with the intensities $I_L = 10^{10}$ W/cm^2 and $I_H = 10^8$ W/cm^2, respectively. The number of photons absorbed refers to the fundamental frequency, for the harmonic field it should be divided by 3. The number in brackets indicates the power of 10.

Number of photons absorbed	One-color fundamental (a.u.)	Two-color (a.u.)				One-color harmonic (a.u.)
		$\delta=0$	$\delta=\pi$	$\delta=\pi/2$	$\delta=-\pi/2$	
8	0.72[−9]	0.53[−8]	0.36[−9]	0.24[−8]	0.25[−8]	
9	0.20[−9]	0.93[−9]	0.18[−9]	0.68[−9]	0.68[−9]	0.30[−13]
10	0.39[−10]	0.25[−9]	0.82[−10]	0.25[−9]	0.22[−9]	
11	0.40[−11]	0.59[−10]	0.65[−10]	0.88[−10]	0.66[−10]	
12	0.71[−12]	0.14[−10]	0.33[−10]	0.28[−10]	0.22[−10]	0.98[−17]
13	0.33[−12]	0.45[−11]	0.13[−10]	0.82[−11]	0.94[−11]	
14	0.14[−12]	0.21[−11]	0.47[−11]	0.24[−11]	0.49[−11]	
15	0.47[−13]	0.11[−11]	0.17[−11]	0.70[−12]	0.25[−11]	
16	0.14[−13]	0.52[−12]	0.60[−12]	0.21[−12]	0.12[−11]	
17	0.35[−14]	0.22[−12]	0.22[−12]	0.64[−13]	0.50[−12]	
Total rate	0.96[−9]	0.66[−8]	0.74[−9]	0.35[−8]	0.35[−8]	0.30[−13]

$$A_n=\sum_m (2\pi)^{-1}\int_{-\pi}^{\pi} d\tau \exp(i(n-m)\tau - i(2\omega)^{-3}\mathbf{F}_1^2\sin 2\tau - i(2p\omega)^{-3}\mathbf{F}_2^2\sin(2p\tau+2\delta)$$
$$+ik_n\hat{\mathbf{r}}\cdot[\omega^{-2}\mathbf{F}_1\cos\tau+(p\omega)^{-2}\mathbf{F}_2\cos(p\tau+\delta)]$$
$$-i(2p\omega^2)^{-1}(\mathbf{F}_1\cdot\mathbf{F}_2)\{[(p+1)\omega]^{-1}\sin[(p+1)\tau+\delta]-[(p-1)\omega]^{-1}\sin[(p-1)\tau+\delta]\})$$
$$\times\int d^3\mathbf{r}'\exp\{-ik_n\hat{\mathbf{r}}\cdot\mathbf{r}'+i\mathbf{r}'\cdot[\omega^{-1}\mathbf{F}_1\sin\tau+(p\omega)^{-1}\mathbf{F}_2\sin(p\tau+\delta)]\}W(r')\psi_m(\mathbf{r}') \ . \quad (30)$$

In Eqs. (29) and (30) $\hat{\mathbf{r}}$ is the unit vector in the direction of the electron ejection.

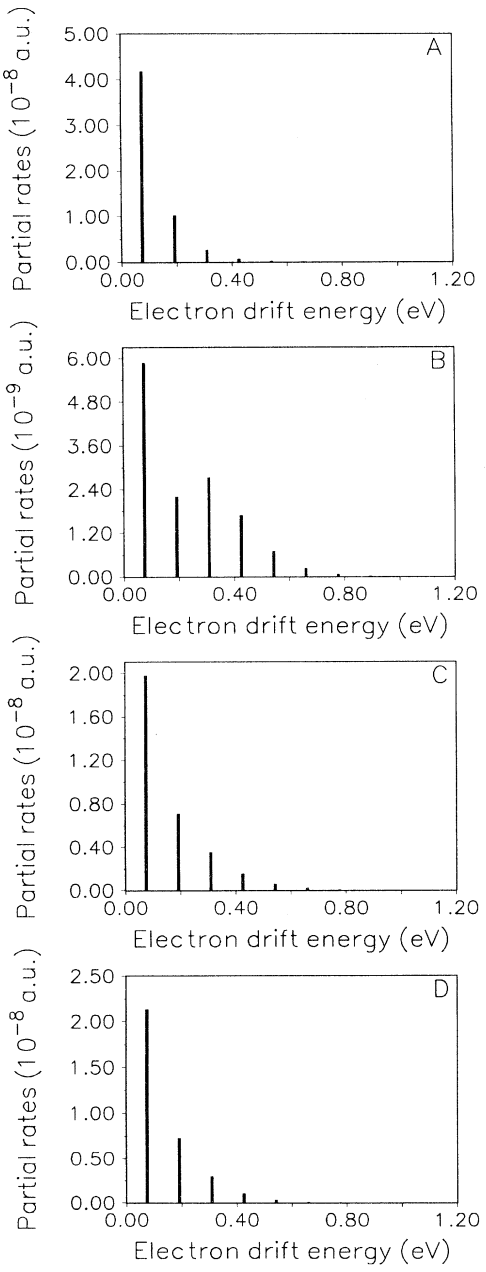

FIG. 1. Electron energy distributions after multiphoton above-threshold detachment from H^- by 10.6-μm radiation and its third harmonic with the intensities $I_L=10^{10}$ and $L_H=10^9$ W/cm^2, respectively. The heights of the bars correspond to the partial rates after absorption of n fundamental frequency photons, starting with $n_{\min}=8$. Phase shift (A) $\delta=0$, (B) $\delta=\pi$, (C) $\delta=\pi/2$, (D) $\delta=-\pi/2$.

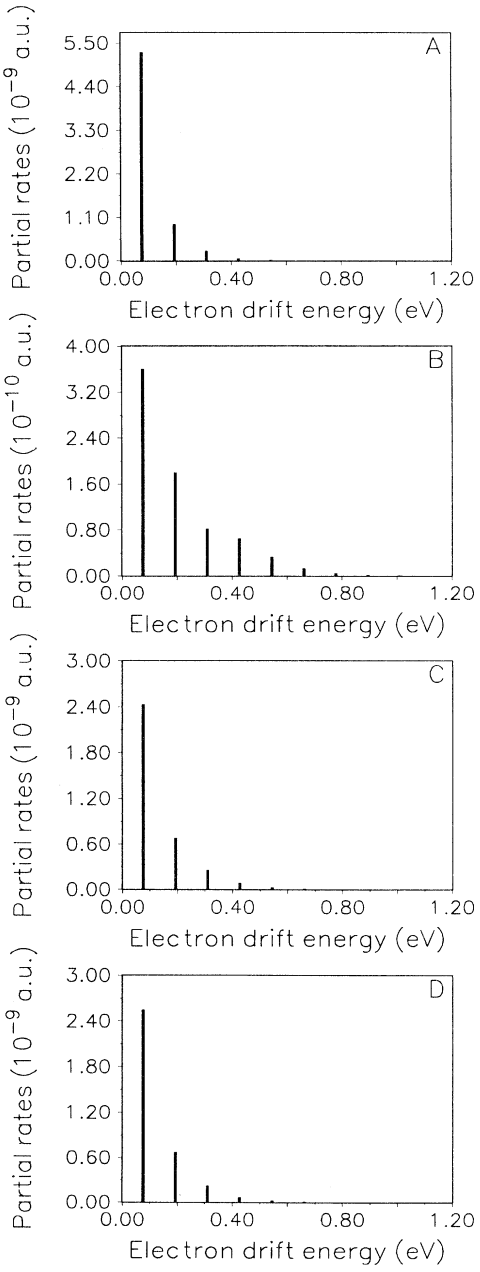

FIG. 2. Electron energy distribution after multiphoton above-threshold detachment from H^- by 10.6-μm radiation and its third harmonic with the intensities $I_L=10^{10}$ and $I_H=10^8$ W/cm^2, respectively. The heights of the bars correspond to the partial rates after absorption of n fundamental frequency photons, starting with $n_{\min}=8$. Phase shift (A) $\delta=0$, (B) $\delta=\pi$, (C) $\delta=\pi/2$, (D) $\delta=-\pi/2$.

III. RESULTS

Expression (30) is general and contains three-dimensional space and one-dimensional time integration. In what follows we consider the special case when the two fields are polarized in the same direction. In this case, for the spherically symmetrical potential $W(r)$, the projection of the electron angular momentum onto the field axis is an integral of motion. Since the H^- ground state is under consideration, this projection is equal to zero. Thus the wave-function Fourier component $\psi_m(\mathbf{r})$ can be expanded in the series over the Legendre polynomials $P_l(\cos\vartheta)$, ϑ being the angle between $\mathbf{r}$ and the field direction:

$$\psi_m(\mathbf{r})=\sum_{l=0}^{\infty}\sqrt{2l+1}\psi_{ml}(r)P_l(\cos\vartheta)\ . \tag{31}$$

It is that form of the wave function which was used in the previous calculations of the wave functions by the CSGPS method [see [13]; the series (31) is truncated to an appropriate value $l_{\max}$ of the angular momentum]. Then the integrations over the angles ϑ and φ (in the spherical coordinate system with the polar axis along the field direction) can be performed analytically, giving the following expression for the photodetachment amplitude A_n instead of (30):

$$\begin{aligned}A_n=\sum_m\int_{-\pi}^{\pi}d\tau\exp(i(n-m)\tau-i(2\omega)^{-3}F_1^2\sin2\tau-i(2p\omega)^{-3}F_2^2\sin(2p\tau+2\delta)\\ -ik_n^{\parallel}[\omega^{-1}F_1\cos\tau+(p\omega)^{-2}F_2\cos(p\tau+\delta)]\\ -i(2p\omega^2)^{-1}F_1F_2\{[(p+1)\omega]^{-1}\sin[(p+1)\tau+\delta]-[(p-1)\omega]^{-1}\sin[(p-1)\tau+\delta]\})\\ \times2\int_0^{\infty}dr\,r^2\sum_{l=0}^{\infty}(-1)^l\sqrt{2l+1}\psi_{ml}(r)W(r)j_l(K_nr)P_l\left[\frac{k_n^{\parallel}-\omega^{-1}F_1\sin\tau-(p\omega)^{-1}F_2\sin(p\tau+\delta)}{K_n}\right]\ .\end{aligned} \tag{32}$$

Here $j_l(x)$ is the spherical Bessel function, $k_n^{\parallel}$ is the projection of the electron drift momentum on the field direction, and K_n is defined as

$$\begin{aligned}K_n=\{(k_n^{\perp})^2+[k_n^{\parallel}-\omega^{-1}\mathbf{F}_1\sin\tau\\ -(p\omega)^{-1}\mathbf{F}_2\sin(p\tau+\delta)]^2\}^{1/2}\ ,\end{aligned} \tag{33}$$

with $k_n^{\perp}$ being the projection of the electron drift momentum on the plane perpendicular to the field direction. The expression (32) is suitable for practical calculations since it contains just two integrations, and the integration over τ can be performed effectively using fast Fourier transform routines for all the numbers of absorbed photons n at the same time.

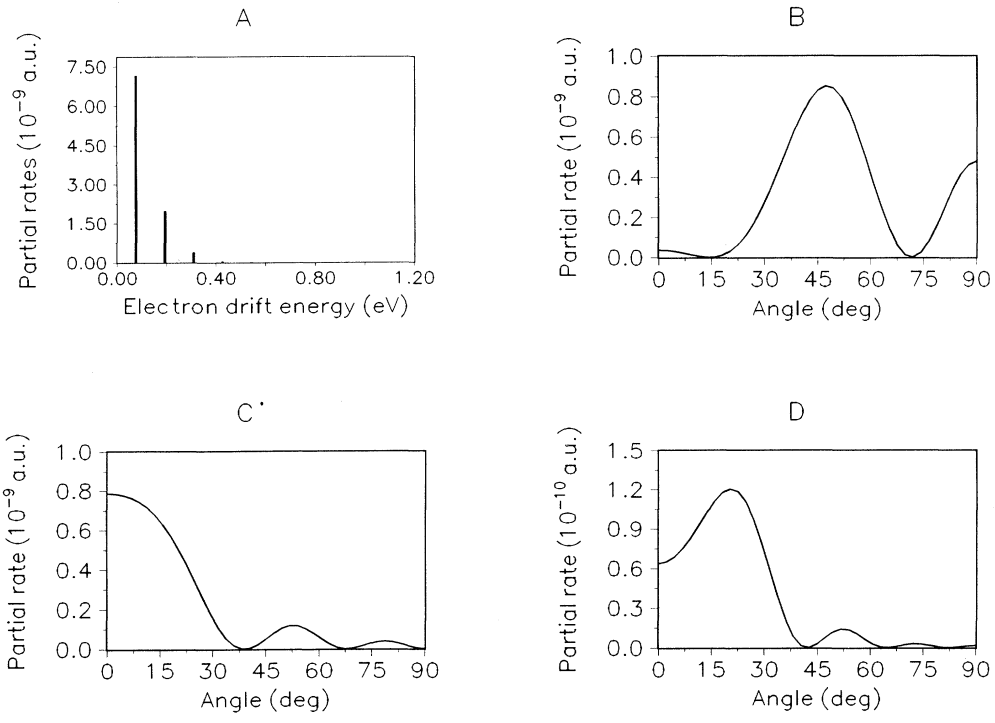

FIG. 3. Electron energy and angular distributions after multiphoton above-threshold detachment from H^- by 10.6-μm radiation alone (the intensity is $I_L=10^{10}$ W/cm^2). (A) The energy spectrum; the heights of the bars correspond to the partial rates after absorption of n photons, starting with $n_{\min}=8$. (B) The angular distribution for the number of photons absorbed, $n=8$. (C) The angular distribution for $n=9$. (D) The angular distribution for $n=10$.

The calculations of electron angular and energy spectra were performed for the fundamental frequency $\omega=4.2984\times10^{-3}$ a.u. corresponding to the wavelength 10.6 μm used in Los Alamos experiments [7–9], and its third harmonic. The fundamental frequency field intensity used is $I_L=10^{10}$ W/cm^2 for all the calculations. The harmonic field intensities were chosen to be $I_H=10^9$ and 10^8 W/cm^2, and the relative phase shifts are $\delta=0,\pi,\pm\pi/2$. The complex quasienergy resonance eigenfunction and eigenvalue corresponding to the H^- ground state are determined by the solution of the non-Hermitian Floquet Hamiltonian using the complex-scaling generalized pseudospectral technique [12]. The number of Legendre grid points used is 40, and a sufficient number of partial waves and Fourier components (up to 17) is used to ensure the convergency of the complex eigenvalues. A computer code using the implicitly restarted Arnoldi algorithm [22] is developed for efficient and accurate solution of the large-scale complex eigenvalue problem. A more detailed presentation of this method will be discussed elsewhere. The partial rates and angular distributions are obtained by the rotation of the complex-scaling wave functions back to the real axis as described in Ref. [13].

The partial and total rates for two-color detachment are presented in Table I for the harmonic field intensity $I_H=10^9$ W/cm^2 and in Table II for $I_H=10^8$ W/cm^2. Also presented there are the results for one-color detachment by the fundamental frequency field and its third harmonic, respectively. One can see that for the rather strong harmonic field ($I_H=10^9$ W/cm^2, Table I) the detachment is dramatically enhanced, compared with the one-color case, for all the phase δ values used in the calculations. However, for the weaker harmonic intensity ($I_H=10^8$ W/cm^2, Table II) and $\delta=\pi$, the total rate is less than that for the one-color detachment by the fundamental field. Thus the small admixture of the harmonic field can lead to the relative stabilization of the H^- ion against the multiphoton detachment. The dependence of the total rate on the relative phase shift δ is the same for both strong and weak harmonic fields. The greatest rate is observed for $\delta=0$, and the smallest for $\delta=\pi$. These results are in qualitative agreement with the previous calculations for atomic hydrogen [3]. The phase shifts $\delta=\pm\pi/2$ give the intermediate total rate values which seem to be the same within the computation error. The latter fact is quite surprising since the Schrödinger equation (1) has no symmetry with respect to time reversal. However, for the field intensities used in the calculations we did not observe any significant difference between $\delta=\pi/2$ and $\delta=-\pi/2$ for the total rate while the partial rates and angular distributions show well-pronounced difference.

If the detachment process corresponds to the tunneling regime, these results can be explained by a simple argument that the electric field peak value is maximal for $\delta=0$ and minimal for $\delta=\pi$, and the tunneling detachment rate depends strongly (exponentially) on the electric field peak value. On the other hand, in the multiphoton detachment regime the phase dependence of the total and partial rates can be described as a result of interference among various pathways leading to the same final state in the continuum. From this point of view it is clear that neither the absorption of the fundamental frequency photons only nor that of the harmonic frequency is effective

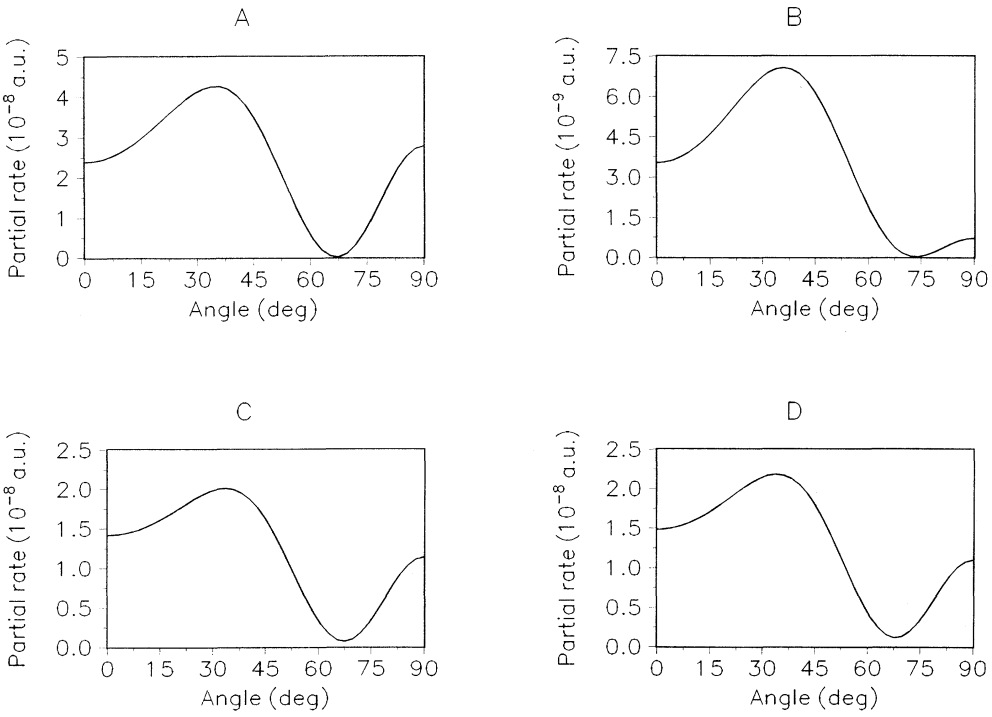

FIG. 4. Electron angular distributions $(1/\sin\vartheta)d\Gamma/d\vartheta$ for the eight-photon peak in the energy spectrum. Graphs A–D correspond to detachment by 10.6-μm radiation and its third harmonic with the intensities $I_L=10^{10}$ and $I_H=10^9$ W/cm^2 and phase shifts (A) $\delta=0$, (B) $\delta=\pi$, (C) $\delta=\pi/2$, (D) $\delta=-\pi/2$.

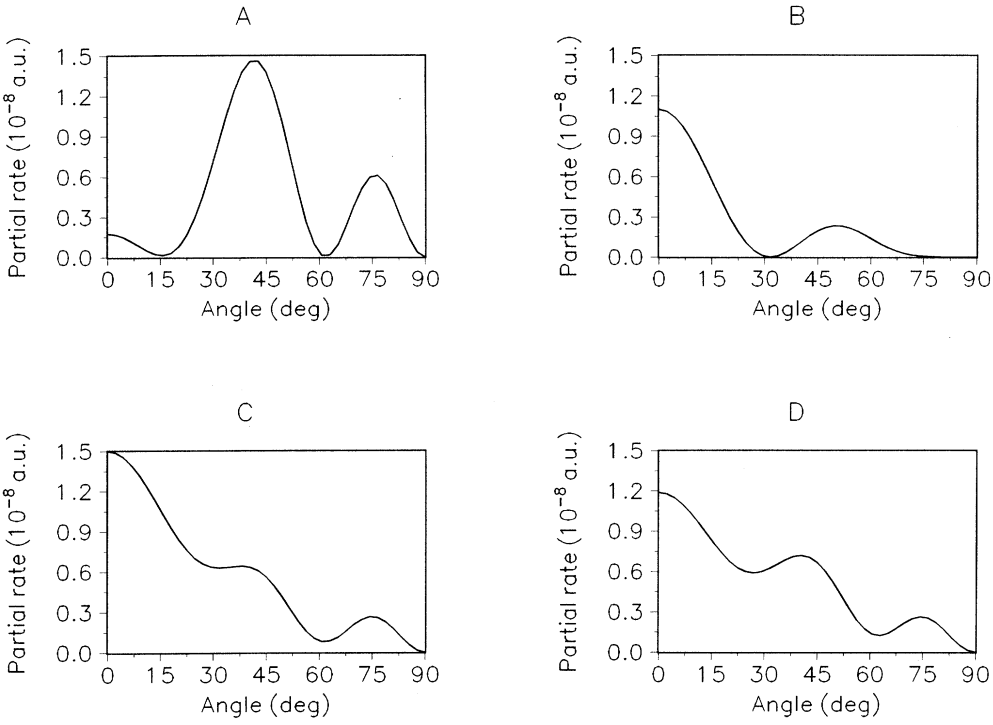

FIG. 5. The same as Fig. 4 for the nine-photon above-threshold peak in the energy spectrum.

for the detachment since the corresponding rates for the one-color detachment are much less than that for the two-color detachment. However, for the parameters used in the calculations the detachment regime is neither pure tunneling nor multiphoton but intermediate, so both pictures can be applied to some extent.

The energy spectra are presented in Figs. 1 and 2 for various harmonic field intensities and relative phases. Compared to the case of one-color detachment by the fundamental frequency field with the same intensity [Fig. 3(A)], one can see more above-threshold peaks of significant intensity in the two-color case. This

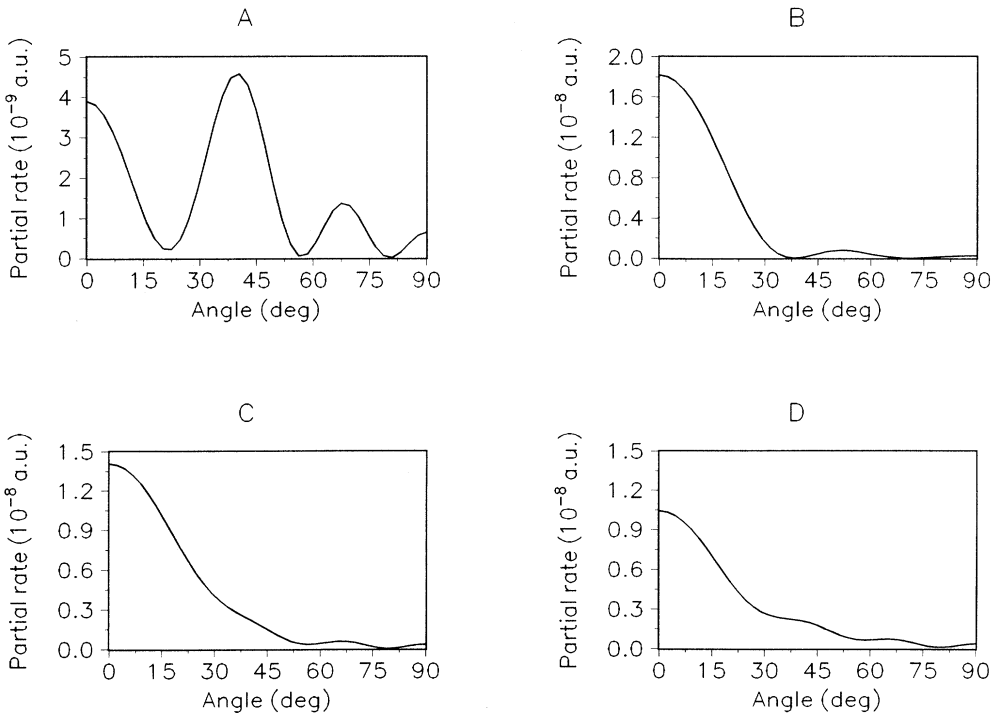

FIG. 6. The same as Fig. 4 for the ten-photon above-threshold peak in the energy spectrum.

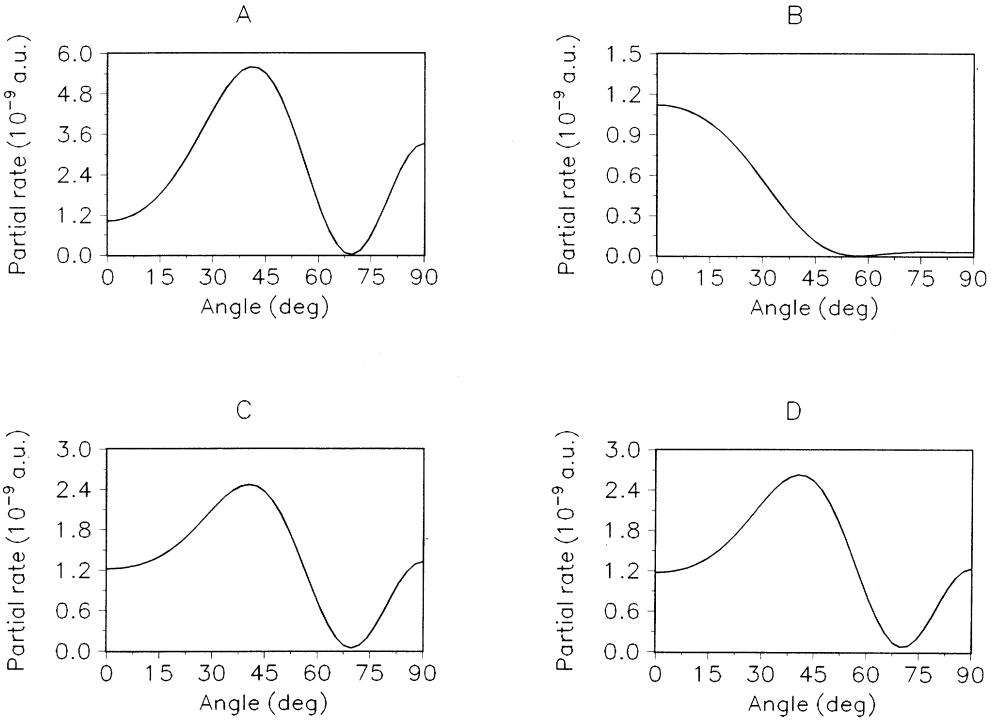

FIG. 7. Electron angular distributions $(1/\sin\vartheta)d\Gamma/d\vartheta$ for the eight-photon peak in the energy spectrum. Graphs A–D correspond to detachment by 10.6-μm radiation and its third harmonic with the intensities $I_L=10^{10}$ and $I_H=10^8$ W/cm^2 and phase shifts (A) $\delta=0$, (B) $\delta=\pi$, (C) $\delta=\pi/2$, (D) $\delta=-\pi/2$.

phenomenon was observed earlier by Yao and Chu [23] for the one-dimensional δ-function model of a negative ion.

The results for the case of fundamental field intensity $I_L=10^{10}$ W/cm^2 and harmonic field intensity $I_H=10^9$ W/cm^2 are presented in Fig. 1, for the phase shifts $\delta=0,\pi,\pm\pi/2$. The maximum in the energy spectrum still corresponds to the first (eight-photon) peak, as for the one-color detachment [Fig. 3(A)]. For $\delta=0$ [Fig. 1(A)] the spectrum envelope is quite narrow and similar to that of the one-color detachment (only the first three to four peaks contribute significantly to the total rate).

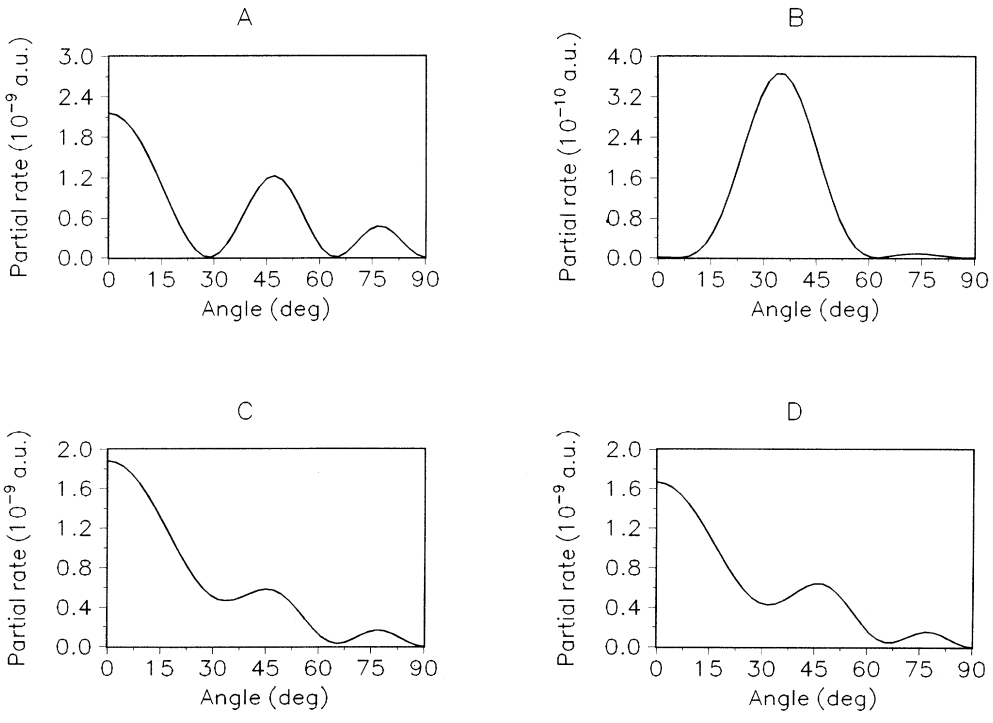

FIG. 8. The same as Fig. 7 for the nine-photon above-threshold peak in the energy spectrum.

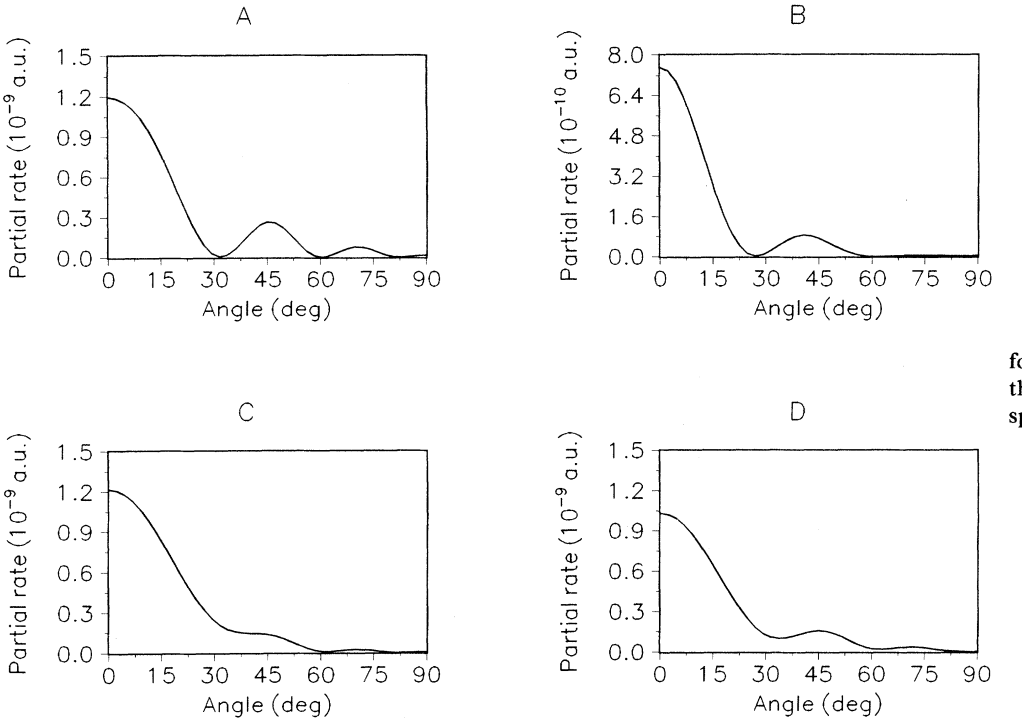

FIG. 9. The same as Fig. 7 for the ten-photon above-threshold peak in the energy spectrum.

For $\delta=\pm\pi/2$ [Figs. 1(C) and 1(D)] the envelope becomes broader (five to six peaks are important), and for $\delta=\pi$ [Fig. 1(B)] one can see even the second maximum in the energy spectrum corresponding to absorption of $n=10$ photons. In the latter case ($\delta=\pi$) the spectrum is the broadest while the total rate is the smallest.

For the fundamental field intensity $I_L=10^{10}$ W/cm^2 and the harmonic field intensity $I_H=10^8$ W/cm^2 (Fig. 2), the behavior of the energy spectra is similar to that for the intensity $I_H=10^9$ W/cm^2: the narrowest envelope appears for $\delta=0$ [Fig. 2(A)], the broadest one for $\delta=\pi$ [Fig. 2(B)]. However, in contrast to the case of the stronger harmonic field, the energy spectrum for $\delta=\pi$ [Fig. 2(B)] is decreasing monotonously, it has just one maximum corresponding to the first (eight-photon) peak.

The analysis of the electron angular distributions for the harmonic intensity $I_H=10^9$ W/cm^2 (Figs. 4, 5, and 6 corresponding to the absorption of eight, nine, and ten photons, respectively) can explain the behavior of the energy spectra. For a high order nonlinear process the most effective detachment occurs when the electrons are ejected along the polarization direction of the external field. That is why the angular distributions are generally peaked in some angular range around the field direction if they correspond to absorption of a large number of photons. The interference between the fundamental and harmonic fields can redistribute the electron ejection in various directions. For the first peaks in the energy spectrum this interference is constructive for $\delta=0$ and destructive for $\delta=\pi$ in the angular range around the field direction (see Fig. 5). This circumstance determines the larger total rate for $\delta=0$ since the first peaks make the most significant contribution to the total rate. However, with the increasing number of absorbed photons the interference in the field direction becomes destructive for $\delta=0$ and constructive for $\delta=\pi$ (see Figs. 5 and 6). It is reflected also in a broader energy spectrum envelope for $\delta=\pi$ and larger partial rates compared to the case $\delta=0$, for the large number of absorbed photons (see Table I).

The analogous angular distributions for the harmonic field intensity $I_H=10^8$ W/cm^2 are shown in Figs. 7–9. Again, the interference of different paths leading to the final states with the same energy in the continuum appreciably redistributes the ejected electrons in various directions. However, the destructive interference for $\delta=\pi$ is manifested here for more peaks in the energy spectrum, and not only for the ejection angles close to the field direction. That is why the total rate for $\delta=\pi$ is not only less than that for $\delta=0$, but also less than the total rate for the one-color detachment.

IV. CONCLUSION

In this paper we have presented a nonperturbative study of the angular distributions and partial widths for multiphoton above-threshold detachment of the H^- ion by 10.6-μm radiation and its third harmonic. The general theory of electron distributions after two-color detachment based on the integral equation (19) (or its counterpart for commensurable frequencies) enables us to obtain the distributions via a quite simple and yet stable and efficient numerical procedure. The wave functions used by this procedure are computed by means of the non-Hermitian Floquet theory and the generalized complex-

scaling pseudospectral discretization technique.

The results for the total and partial rates and angular distributions show the following general trend. First, the total and partial rates for the two-color detachment, when the intensity of the harmonic field is 10 and 100 times less than that of the fundamental frequency field, are generally much larger than the rates for the one-color detachment by the fundamental frequency or the harmonic alone. However, the opposite situation is also possible if the harmonic field is weak enough and the relative phase shift is close to π. Second, the total and partial rates manifest a strong dependence on the relative phase between the two fields. The total rate is the largest for the phase $\delta=0$ and the smallest for $\delta=\pi$. For the weak harmonic field and $\delta=\pi$ it can be even less than the total rate for the fundamental field alone. Hence the small admixture of the harmonic field can lead to relative stabilization of H^- ions against decay in the laser field. Such a dependence on the relative phase shift is also valid for the first few partial rates (i.e., for the heights of the first few peaks in the energy spectrum). However, for the subsequent above-threshold peaks the picture is completely different: the largest partial rates correspond to $\delta=\pi$ and the smallest ones correspond to $\delta=0$. In other words, the decrease of the partial rates with their number is slower for $\delta=\pi$ than for $\delta=0$. Third, the angular distributions also exhibit strong phase dependence. For the first (eight-photon) peaks in the energy spectra they show relative suppression of detachment at the small angles if $\delta=\pi$ whereas for a larger number of absorbed photons such a suppression occurs for $\delta=0$.

It seems that the features of two-color detachment mentioned above have a general kinematic nature related to the motion of the electron in the two-color laser field since they are generated mostly by the Green function for the motion in the laser field and do not depend qualitatively on the atomic potential. This conclusion is confirmed also by the similar results for the atomic hydrogen (total rates) [3,4].

ACKNOWLEDGMENTS

This work was partially supported by the Division of Chemical Sciences, Office of Basic Energy Sciences of the U.S. Department of Energy. We are grateful to Dr. D. C. Sorensen for providing a complex version of the ARPACK computer program used. One of us (D.A.T.) acknowledges also the partial financial support from the International Science Foundation (Individual Grants Program for the former Soviet Union).

[1] H. G. Muller, P. H. Buskbaum, D. W. Schumacher, and A. Zavriyev, J. Phys. B **23**, 2761 (1990); C. Chen and D. S. Elliot, Phys. Rev. Lett. **65**, 1737 (1990).

[2] K. J. Schafer and K. C. Kulander, Phys. Rev. A **45**, 8026 (1992).

[3] R. M. Potvliege and P. H. G. Smith, J. Phys. B **24**, L641 (1991).

[4] R. M. Potvliege and P. H. G. Smith, J. Phys. B **25**, 2501 (1992).

[5] R. M. Potvliege and P. H. G. Smith, Phys. Rev. A **49**, 3110 (1994).

[6] M. Pont, D. Proulx, and R. Shakeshaft, Phys. Rev. A **44**, 4486 (1991).

[7] C. Y. Tang, P. G. Harris, A. H. Mohagheghi, H. C. Bryant, C. R. Quick, J. B. Donahue, R. A. Reeder, S. Cohen, W. W. Smith, and J. E. Stewart, Phys. Rev. A **39**, 6068 (1989).

[8] W. W. Smith, C. Y. Tang, C. R. Quick, H. C. Bryant, P. G. Harris, A. H. Mohagheghi, J. B. Donahue, R. A. Reeder, H. Sharifian, J. E. Stewart, H. Toutounchi, S. Cohen, T. C. Altman, and D. C. Rislove, J. Opt. Soc. Am. B **8**, 17 (1991).

[9] C. Y. Tang, P. G. Harris, H. C. Bryant, A. H. Mohagheghi, R. A. Reeder, H. Sharifian, H. Toutounchi, C. R. Quick, J. B. Donahue, S. Cohen, and W. W. Smith, Phys. Rev. Lett. **66**, 3124 (1991).

[10] For a summary of recent work and a more complete list of references in this direction, see S. Geltman, Phys. Rev. A **43**, 4930 (1991); see also C. R. Liu, B. Gao, and A. F. Starace, *ibid.* **46**, 5985 (1992).

[11] C. Laughlin and S. I. Chu, Phys. Rev. A **48**, 4654 (1993).

[12] J. Wang, S. I. Chu, and C. Laughlin, Phys. Rev. A **50**, 3208 (1994).

[13] D. A. Telnov and S. I. Chu, Phys. Rev. A **50**, 4099 (1994).

[14] K. R. Lykke, K. K. Murray, and W. C. Lineberger, Phys. Rev. A **43**, 6104 (1991).

[15] C. Schwartz, Phys. Rev. **124**, 1468 (1961); A. L. Stewart, J. Phys. B **11**, 3851 (1978); M. R. H. Rudge, *ibid.* **8**, 940 (1975); J. Callaway, Phys. Rev. **65A**, 199 (1978).

[16] A. W. Wishart, J. Phys. B **12**, 3511 (1979); A. L. Stewart, *ibid.* **11**, 3851 (1978).

[17] G. Yao and S. I. Chu, Chem. Phys. Lett. **204**, 381 (1993).

[18] S. I. Chu and W. P. Reinhardt, Phys. Rev. Lett. **39**, 1195 (1977); A. Maquet, S. I. Chu, and W. P. Reinhardt, Phys. Rev. A **27**, 2946 (1983).

[19] For reviews on non-Hermitian Floquet Hamiltonian methods, see S. I. Chu, Adv. At. Mol. Phys. **21**, 197 (1985); Adv. Chem. Phys. **73**, 739 (1989).

[20] D. A. Telnov, J. Phys. B **24**, 2967 (1991); V. N. Ostrovsky and D. A. Telnov, *ibid.* **20**, 2397 (1987).

[21] T. S. Ho, S. I. Chu, and J. V. Tietz, Chem. Phys. Lett. **96**, 464 (1983); T. S. Ho and S. I. Chu, J. Phys. B **17**, 2101 (1984).

[22] D. C. Sorensen (private communication).

[23] G. Yao and S. I. Chu, J. Phys. B **25**, 363 (1992).